

**Title of Investigation:** Adaptive Optics System for 1.6 Meter Solar Telescope in Big Bear

**Principal Investigator:** Haimin Wang, BBSO/NJIT

**Co-Principal Investigators:** Phil Goode, Deqing Ren and Carsten Denker, BBSO/NJIT

**Collaborator:** Thomas Rimmele, National Solar Observatory

### **Project Summary**

New Jersey Institute of Technology (NJIT), in collaboration with the University of Hawaii (UH) and the Korean National Observatory, is building the world's largest aperture solar telescope, the 1.6-m aperture New Solar Telescope (NST) to replace Big Bear Solar Observatory (BBSO)'s principal telescope with its 65-cm aperture. The project is well under the way, the telescope is anticipated to have its first light in the end of 2006. Under a prior NSF/MRI support to NJIT, in collaboration with the National Solar Observatory, we have successfully developed two 76-element Adaptive Optics systems (AO-76) for the current BBSO 65-cm telescope and the NSO 76-cm Dunn Telescope.

To fully utilize the scientific capability of NST as soon as possible, we propose to build an AO system by transferring the AO-76 system to NST immediately after the telescope is installed. This proposal seeks funding for this task. The AO-76 is a high-order system for the 65-cm BBSO telescope, which is successfully operating in both the visible and near infrared (NIR) ranges. We understand that, when integrated to NST, the AO-76 will be a lower order AO in the visible. However, we anticipate that it will have full capability to correct the seeing in the NIR. More specifically, under the median seeing condition at BBSO, the predicted Strehl ratio at  $1.6\mu\text{m}$  is above 0.8. For about 10% of the time, the predicted Strehl ratio at  $0.5\mu\text{m}$  is above 0.5. Therefore, our initial scientific focus for NST will be in NIR research of solar atmosphere and its activity. Diffraction limited observations will also be made during the good seeing periods in the visible. The key tasks in this proposal includes the optical design and subsequent setup/test of the AO system for NST. Both the refractive and reflective designs will be considered.

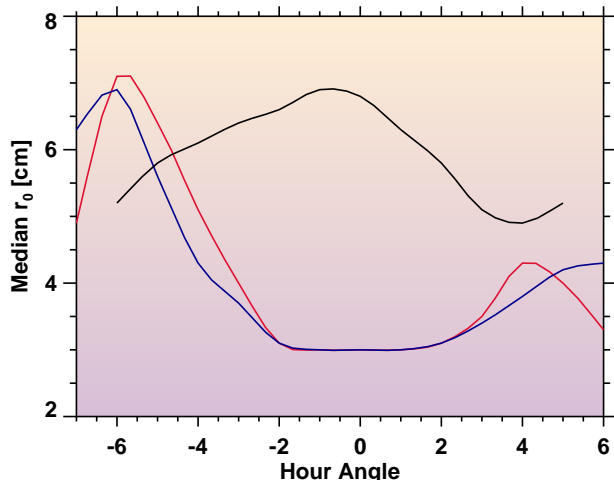
In the last two years, we have developed a state-of-art NIR imaging magnetograph system (IRIM) that has obtained its first scientific light at BBSO. The specific scientific objectives are: (1) High cadence, high resolution studies of solar flares; (2) Evolution of magnetic fields associated with solar activity; and (3) Dynamics of Kilo-gauss magnetic flux tubes.

In sum, we directly address two criteria required in an NSF proposal:

(1) Intellectual merit: The AO equipped NST will be the largest aperture solar telescope, located in one of the best observing sites. It will enable new, cutting edge science. Previous research has already demonstrated our ability by development of the two most successful solar AO systems in the world.

(2) Broad Impact: The development of the proposed AO system is the first solid step toward an even higher-order AO system for the NST, which will also enable us to further explore Multi-Conjugate Adaptive Optics (MCAO). This is highly relevant to the development of MCAO systems for the nighttime telescopes. The scientific results will be extremely important in the understanding of the dynamics of magnetic fields on a fine spatial scale, as well as space weather monitoring and forecasting. The scientific objectives will also be closely linked to several key research topics in nighttime astronomy: the physics of stellar coronal heating, stellar magnetic fields and stellar flares. This project has strong integrated research and education impacts. A post-doc, a Ph.D. student and an undergraduate will participate in the project. Our data will be open to the scientific community.

Figure 1: The median value of the  $r_0$  (Fried parameter, a rough measure of the diffraction limit,  $r_0 \geq 5.5$  cm is required for correction by AO) measurements from the S-DIMM instrument (principal site survey instrument, see <http://atst.nso.edu/site/> for details) for the three finalists to be the ATST site (**Big Bear**, **Haleakala**, and **La Palma**) as a function of hour angle (adapted from Figure 10.13 in Hill et al. 2004, ATST Site Survey Report).



## A. Project Description

### A.1. Results from Prior NSF Support Related to this Proposed Research

Of the two US observatories capable of making high-resolution observations of the Sun, BBSO is the one operating in a campaign mode. We believe that a more fundamental understanding of solar magnetic fields and the solar atmosphere depends on sustained, higher resolution and higher cadence observations. Over the past few years, we have substantial accomplishments that position us to advance to the next level of our scientific objectives, which will center on understanding energy release and transport on different scales in the solar atmosphere, as well as the associated evolution of magnetic fields. Our research requires a continuing effort in instrument development, and a dedicated scientific team to make and analyze new observations. Building the new 1.6-m telescope at BBSO is a crucial step towards this goal.

The Advanced Technology Solar Telescope (ATST) site survey was initiated in 2000 and has identified at the end of a four-year survey three excellent sites for solar observing: Big Bear Solar Observatory, California – Mees Solar Observatory, Haleakala, Maui, Hawaii – Observatorio Roque de los Muchachos, La Palma, Canary Islands, Spain (Hill et al. 2004). All three sites are suitable for high-spatial resolution observations. Haleakala and La Palma have strong advantages for coronal science. However, only BBSO – the mountain-lake site – provides consistent seeing conditions with extended periods of excellent seeing from sunrise to sunset (see Figure 1). For any ground-based modern solar telescope, an Adaptive Optics (AO) system is required to correct seeing induced image smearing and distortions. A minimum Fried parameter, 6cm, is required for AO correctibility. Obviously, BBSO is uniquely qualified to be a site for building a large aperture solar telescope and achieving diffraction limited resolution with AO for long periods of time. Periods of excellent seeing (sufficient to be corrected by AO) are limited to one or two hours in the early morning for the Pacific/Atlantic mountain-island sites Haleakala/La Palma, where the seeing deteriorates once the ground heats up and a turbulent boundary layer has been established. Haleakala was selected as the ATST site to achieve its primary scientific objectives: extreme fine structure of magnetic fields that can be studied with exceptional seeing for short periods of time and physics of solar corona. The lake at BBSO effectively suppresses the boundary layer and makes the observatory ideally suited for sustained high-resolution and synoptic observing programs, and the 1.6-m NST is being built for this purpose.

We now report on the significant progresses on two major instrumentation projects that are relevant to the proposed development of the proposed AO system: the on-going NST project and finished 76-element AO project.

### **A.1.1. New Solar Telescope at BBSO**

Supported by a current NSF MRI grant (ATM-0320540), BBSO/NJIT, in collaboration with the University of Hawaii (UH) and Korean Astronomical Observatory (KAO), have teamed to upgrade BBSO by replacing its principal 65-cm aperture telescope with a modern, off-axis 1.6-m clear aperture instrument with a  $180'' \times 180''$  field of view (FOV) (Goode et al., 2003). The new telescope offers a significant improvement in ground-based high angular resolution capabilities, and enhances our continuing program to understand photospheric magneto-convection and chromospheric dynamics. These are the drivers for what is broadly called space weather – an important problem, which impacts human technologies and life on Earth. This New Solar Telescope (NST) requires a new, larger dome with louvers to ensure proper airflow inside the dome, so the long-standing dome-seeing problem at BBSO can be solved. The NST optical and software control designs are similar to the existing SOLAR-C (UH) and the planned ATST facility led by NSO – all three are off-axis designs. We have full funding for the NST, except the funding for its AO system. Figure 2 shows the mechanical schematics and optical layout of NST. Full operation is expected by the spring of 2007. The specific progresses are:

1. All optical and mechanical designs are completed.
2. The primary mirror is being polished at Steward Observatory Mirror Lab and scheduled for completion no later than February 2006.
3. The secondary mirror and a backup are also in the final polishing stages at SORL.
4. MFG Ratech has been contracted to design and build the new dome. The installation is scheduled for November 2005.
5. Development of the software for the telescope control system is about halfway finished. The communication links between software modules have been written and tested and the development continues on the various subsystem control segments.
6. DFM has been contracted to build the Optical Support Structure and Equatorial Mount.
7. Focal plane instruments for NST are in the final stages of development. These include visible and near infrared magnetograph and real time speckle imaging systems. They are being used to observe with the existing 65-cm telescope.

### **A.1.2. Adaptive Optics**

Under a prior NSF MRI grant (AST-0079482), we have successfully built two high-order AO systems (76 element deformable mirror AO systems), one for BBSO's 65 cm telescope and the other for the 76 cm Dunn Solar Telescope at National Solar Observatory/Sacramento Peak (NSO/SP). Dr. Thomas Rimmele of NSO, as a research professor at NJIT, was the PI for the project. He will participate in this proposed project as a collaborator. A number of papers have been published to describe these two AO systems and the scientific results (Ren et al., 2003a; Didkovsky et al., 2003; Denker et al., 2005; Rimmele, 2004; Yang et al., 2004; Tritschler et al., 2005; Xu et al., 2004, 2005). We present the following images to demonstrate that AO systems work extremely well. Figure 3 is the sample visible and NIR images obtained with the NSO/SP AO system, during the X10 flare on 2003 October 29 (Xu et al., 2004, 2005). This was the first time that a white-light flare is observed in the opacity minimum at  $1.6\mu\text{m}$ . Figure 4 shows a sample image obtained on April 29, 2005 with the BBSO AO system. The performance of the BBSO AO system is evaluated in Figure 5. It compares the variances of the Zernike coefficients for modes up to order 35, for open- and closed-loop data (Tritschler et al., 2005). The variances are a factor of 100 smaller for the AO-corrected data.

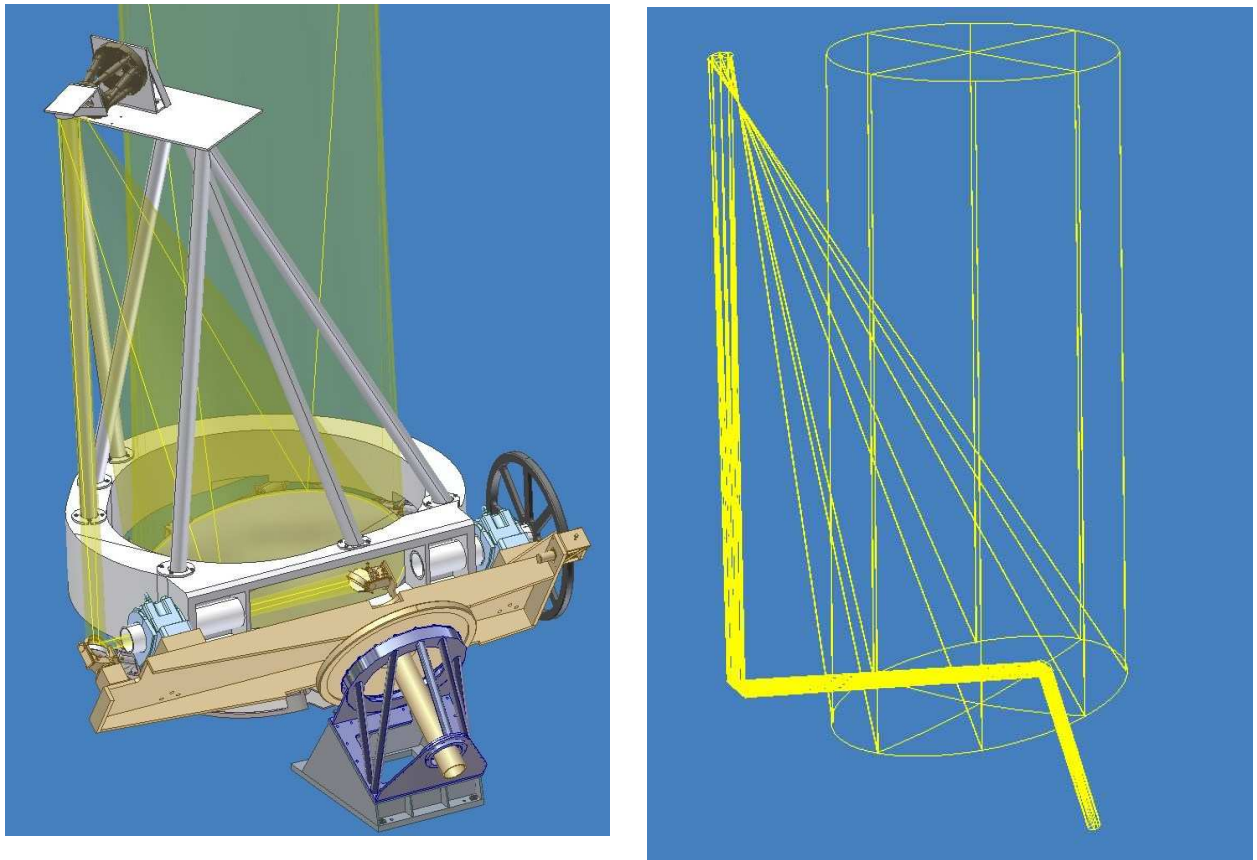


Figure 2: Schematic of the 1.6 m off-axis, open NST and its optical layout.

## A.2. Science Drivers for the AO equipped NST

As we stated above, our initial scientific objectives for the AO equipped NST will be based on achieving full seeing correction in the NIR. In addition, partial correction in the visible will be implemented under good seeing conditions. We therefore emphasize our scientific goals based on continuous NIR observations and periods of visible observations.

BBSO has built and employed a few generations of near IR imaging systems. The most recent and significant part of our IR instrumentation was the development of a narrow bandpass filter system, which combines a Lyot filter and an IR Fabry-Pérot filter – the IR Imaging vector Magnetograph (IRIM). Our one-of-a-kind Lyot filter, designed by one of our former Ph.D. students, has a bandpass of  $2.5 \text{ \AA}$  at  $1.56 \mu\text{m}$ , giving us a  $2.5 \text{ \AA}$  wide prefilter (narrower than the  $5 \text{ \AA}$  free spectral range of the IR Fabry-Pérot). This solves the longstanding problem of constructing a filter-based IR magnetograph, while avoiding the complications of using a double etalon. The new and unique Lyot prefilter is being used in conjunction with our IR Fabry-Pérot filter. With this, polarimetry in the near IR has the same reliability and stability that it has for visible light. Note that the IR Lyot filter system has about 20% transmission. IRIM's total transmission is about a factor of two less than that of a dual Fabry-Pérot instrument. However, unlike a dual Fabry-Pérot system, with its instability (requires very accurate tuning that is hard to maintain) and its typically quite restricted FOV for magnetograms, our system is stable and can utilize larger FOV. Finally, a new detector technology (CMOS devices) offers high quantum efficiency, so that we can take individual exposures well

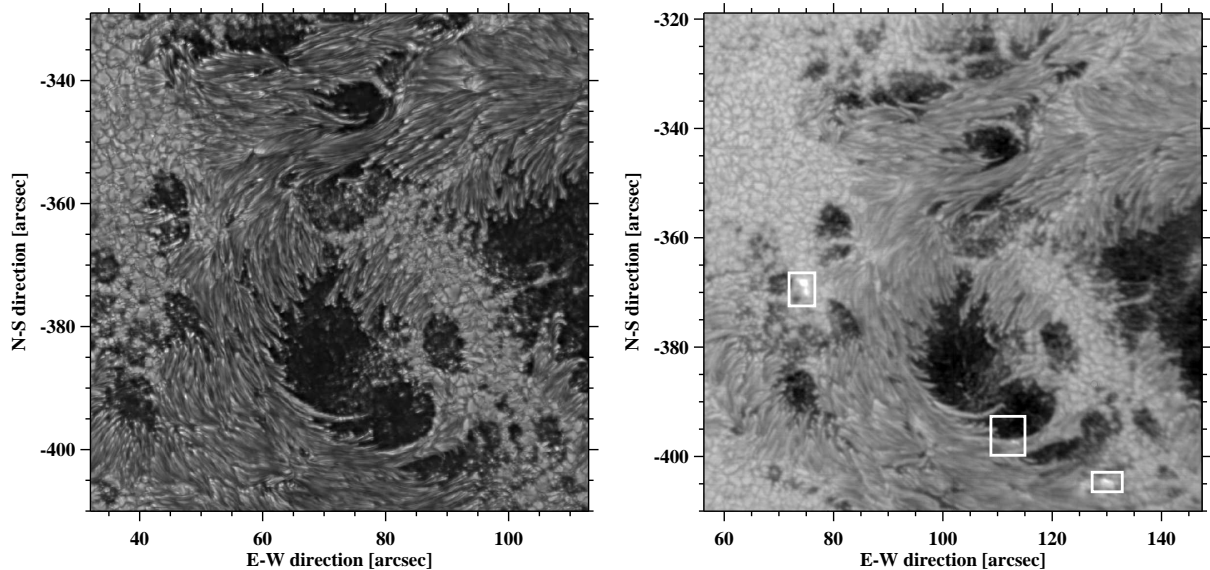


Figure 3: Left Panel: Speckle reconstructed image of active region NOAA 10486 obtained with frame selection and high-order AO system at 16:48 UT on 2003 October 29, at NSO/SP. The annotation of the axes refers to heliographic coordinates corresponding to a FOV of  $81'' \times 81''$ . Right Panel: NIR image of the same active region during the flare taken on 20:42 UT with a FOV of  $91'' \times 91''$ . The bright patches marked by white boxes are NIR flare kernels.

within the atmosphere's correlation time in the near IR ( $\sim 100$  ms). We have obtained and implemented a large format IR CMOS camera ( $1k \times 1k$ , 30 frames/s) from Rockwell Scientific Imaging. We enjoyed a very successful first scientific light of the full IRIM hardware system in November 2004 at NSO/SP and in July 2005 at BBSO. The strength of the IRIM is its extreme sensitivity and high spatial resolution, which allows us to study weak and small-scale magnetic fields in the quiet Sun. In active regions, it allows accurate measurements to avoid Zeeman saturation of the traditional filter-based magnetograph systems. Figures 6 and 7 present example of the IRIM results. Figure 6 compares the BBSO IRIM magnetogram with the corresponding MDI magnetogram. From the sizes of the magnetic structures, it is obvious that IRIM has achieved the diffraction limit ( $0.6$  arcsec at  $1.6\mu m$ ). Figure 7 shows the Stokes V profile and its fitting for a selected point in a new discovered magnetic structure with the IRIM system: the elongated channel structure in the intergranular lanes (Cao et al., 2005). Both magnetic field strength and the filling factor were derived from the fitting of Stokes V profiles.

We are in the process of further upgrading the IRIM system. A second Lyot filter has been built that has a capability to tune from  $1$  to  $1.7\mu m$ . Therefore, we can study solar upper atmosphere with the chromospheric (HeI 1083nm) and coronal (e.g. Fe XIII 1075nm) lines (Lin et al., 2004).

### A.2.1. High Cadence, High Resolution Studies of Solar Flares

The improved resolution from BBSO's NST allows flare imagery and spectroscopy that would otherwise be beyond our reach. High cadence X-ray and microwave observations have revealed a temporal (sub-second) fine structure in solar flares, called elementary flare bursts (see the review paper by Sturrock, 1989). These may be attributed to the fine structure in coronal magnetic fields, which are related to the aggregation of photospheric magnetic fields into "magnetic knots". Recently, the BBSO group has experimented with high cadence flare observations (Wang et al., 2000, Qiu et al., 2000, 2001, 2002, 2005, Ji et al., 2003, 2004a,b),

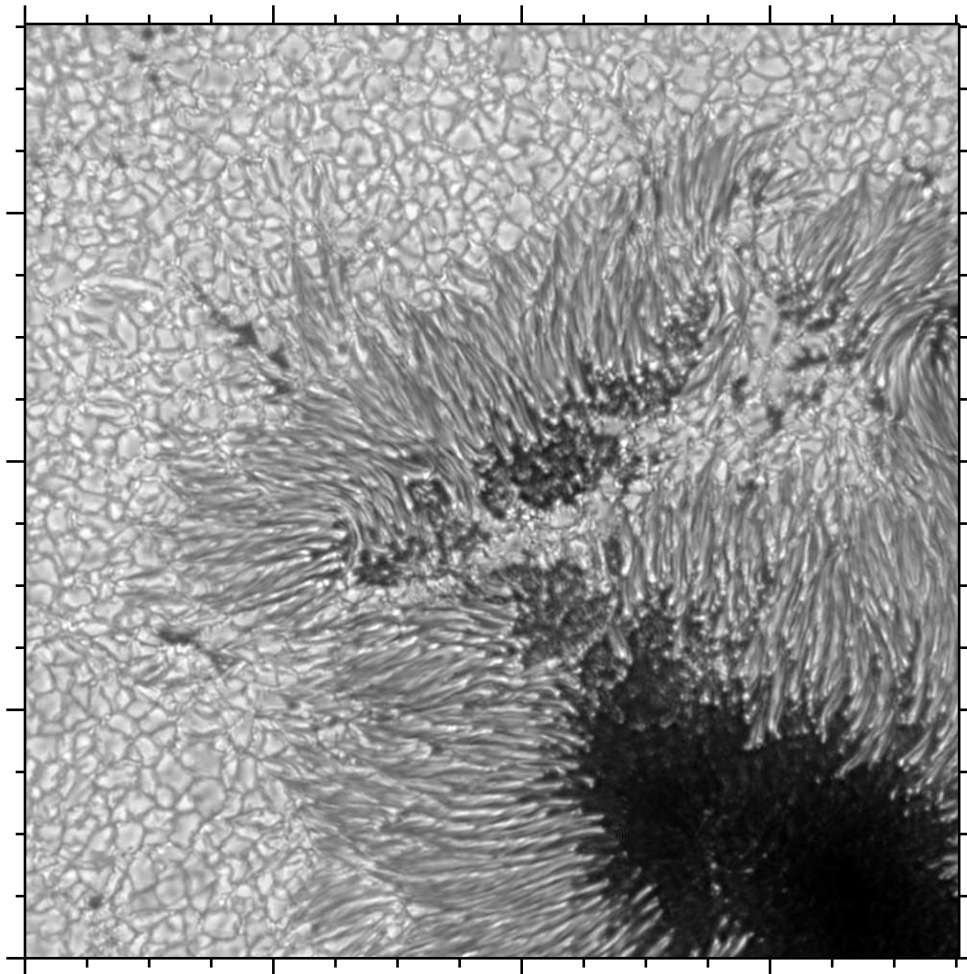


Figure 4: A recent diffraction-limited image obtained at BBSO on April 29, 2005 with the AO-76 system and speckle reconstruction.

probing the far blue wing of  $H\alpha$  with a cadence between 10 ms to 33 ms and an image scale of  $0.5''$ . In particular, Wang et al. (2000) found the  $H\alpha$  source of sub-second hard X-ray bursts. Qiu et al. (2002) studied the footpoint shifts of flare kernels and derived the DC electric current as a function of time. This current was found to be coincident with the hard X-ray temporal profile, and therefore, clearly revealed the flare acceleration mechanism.

The 1.6-m telescope can obtain high resolution, high cadence images of flares in wavelengths such as He D<sub>3</sub> and off-band  $H\alpha$ . These observations will provide details of electron precipitation on fine temporal and spatial scales. By combining high cadence optical imaging with hard X-ray imaging from missions, such as the Ramaty High Energy Solar Spectroscopic Imager (RHESSI), as well as with high resolution magnetograms, we expect to learn if and how the individual sub-second peaks in the hard X-ray and microwave time profiles correlate with the rapid precipitation along various flux loops. Xu et al. (2004, 2005) presented high resolution observations of an X10 white-light flare in solar active region NOAA 10486 obtained with the Dunn Solar Telescope (DST) at the National Solar Observatory/Sacramento Peak (NSO/SP) on 2003 October 29. The investigation focused on flare dynamics observed in the NIR continuum at  $1.56 \mu\text{m}$ . This is the first report of a white-light flare observed at the opacity minimum. The spatial resolution was close to the diffraction limit of the 76 cm aperture DST. The data benefited from the newly developed AO system

Figure 5: Comparison of the variance of the Zernike Coefficients for open (asterisks) and closed-loop (carets) data determined from the AO WFS data. The Solid curve represents a fit to Kolmogoroff spectrum of the open-loop data for  $D/r_0=12.10$  (Trischler et al., 2005).

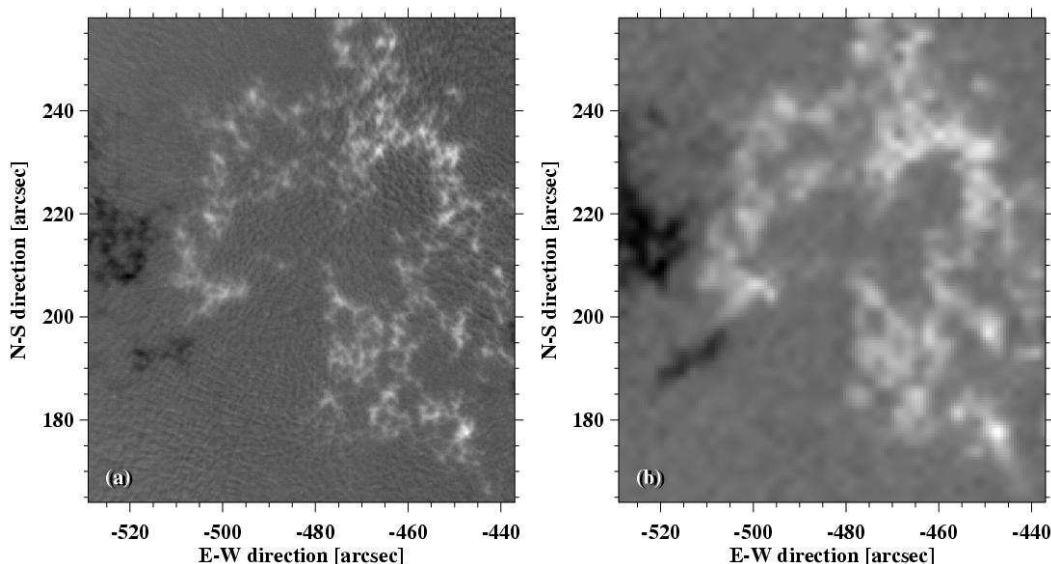
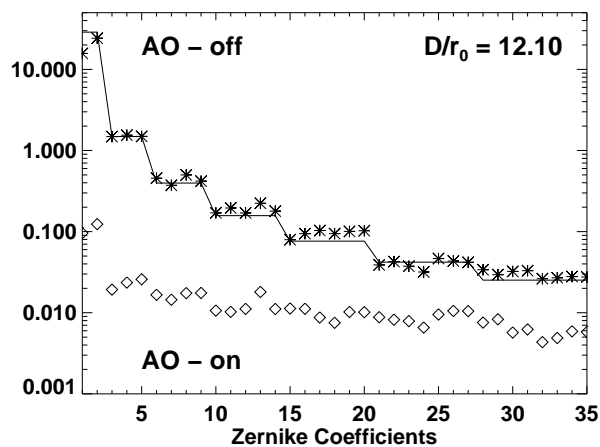


Figure 6: (a): IRIM magnetogram taken at 16:02 UT, on July 1, 2005 with AO-76. (b) MDI magnetogram taken at 16:00 UT.

and the NIR CMOS camera. In addition, we compared hard X-ray (HXR) data of the RHESSI. Although it is still possible that some high energy electrons penetrate deep to this layer, a more likely explanation of the observed emission is back-warming. During the impulsive phase of the flare, two major flare ribbons moved apart, which were both temporally and spatially correlated with RHESSI HXR ribbons. The maximum intensity enhancement of the two flare ribbons is 18% and 25%, respectively, compared to the quiet sun NIR continuum. Figure 8 shows the comparison of NIR flare image and the RHESSI HXR emission contours. It is clear that NIR emissions coincide well with HXR foot point emissions, but NIR observations have much better spatial ( $0.6''$ ) and temporal (30ms) resolutions to understand the fine scale structure of flare footpoints.

Since the 1.6-m telescope will provide a spatial resolution of  $\approx 50$  km in the visible wavelength region, and  $\approx 150$  km in NIR, we will be able to determine whether the moving flare kernels have such a small scale.



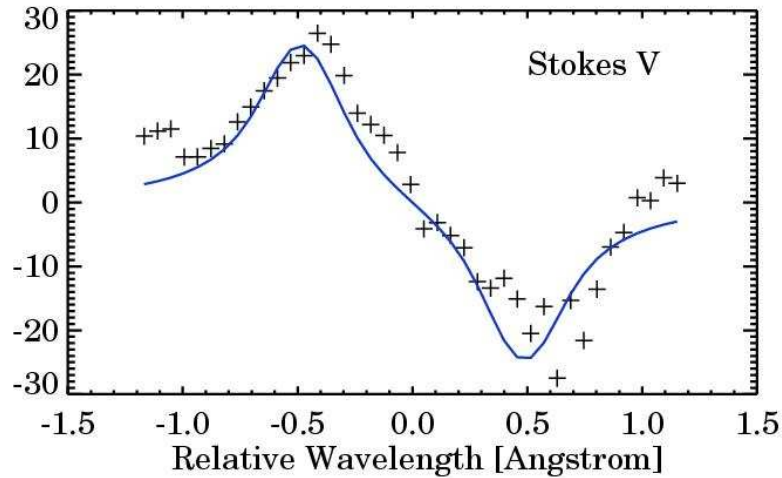


Figure 7: An example of observed and fitted Stokes V profile from the data set shown in Figure 6 (Cao et al, 2005).

### A.2.2. Structure and Evolution of Magnetic Fields and Flow Fields in Flaring Active Regions

The research using the NST will answer the following questions: (a) What is the role of the evolution of the photospheric magnetic field in triggering solar flares, and what is the relationship between the magnetic configuration and the properties of flares? (b) How do electric currents evolve, and what is their relationship to particle precipitation?

It is generally accepted that the energy released in solar flares is stored in stressed magnetic fields. So, the study of magnetic fields is a very important component of flare science. This concept of energy release has motivated many attempts to detect flare-induced changes in the magnetic fields of active regions. Until very recently, no one has detected, in any consistent way, the changes in magnetic fields associated with solar flares. The BBSO group started to see signs of these changes using BBSO, TRACE and MDI one-minute cadence data (Spirock et al., 2002; Wang et al., 2002, 2004, 2005; Liu et al., 2005). The inconsistency among the results is due to observational limitations. We cannot get high temporal and spatial resolution and high polarization accuracy at the same time, with existing telescopes/instruments. Our new, large telescope will provide much more reliable and high quality measurements of vector magnetic fields. A lot of the questions discussed above will be resolved with the new higher resolution, higher cadence data. In addition to the temporal and spatial resolution mentioned earlier, the precision of the polarimetry would be on the order of  $10^{-4}$  for the IRIM. With the improved accuracy of our vector magnetograph system, studies of more examples of evolving magnetic fields in active regions, and changes due to flares will provide the evidence needed to lead us to understanding the process of flare energy release, and the role of photospheric magnetic fields therein.

In addition to the structure of magnetic fields, we understand that the flows play an important role in understanding the triggering of solar flares. This needs to be studied with two dimensional flow fields derived by local correlation tracking. To observe these flows and magnetic field structure in detail and to understand their basic nature, we need high-resolution and high-cadence observations. AO equipped NST will help achieve breakthroughs by finally advancing us beyond the current resolution limit. Yang et al. (2004) compared the flow directions and flare footpoints, the shear flows are very obviously associated with flaring neutral lines.



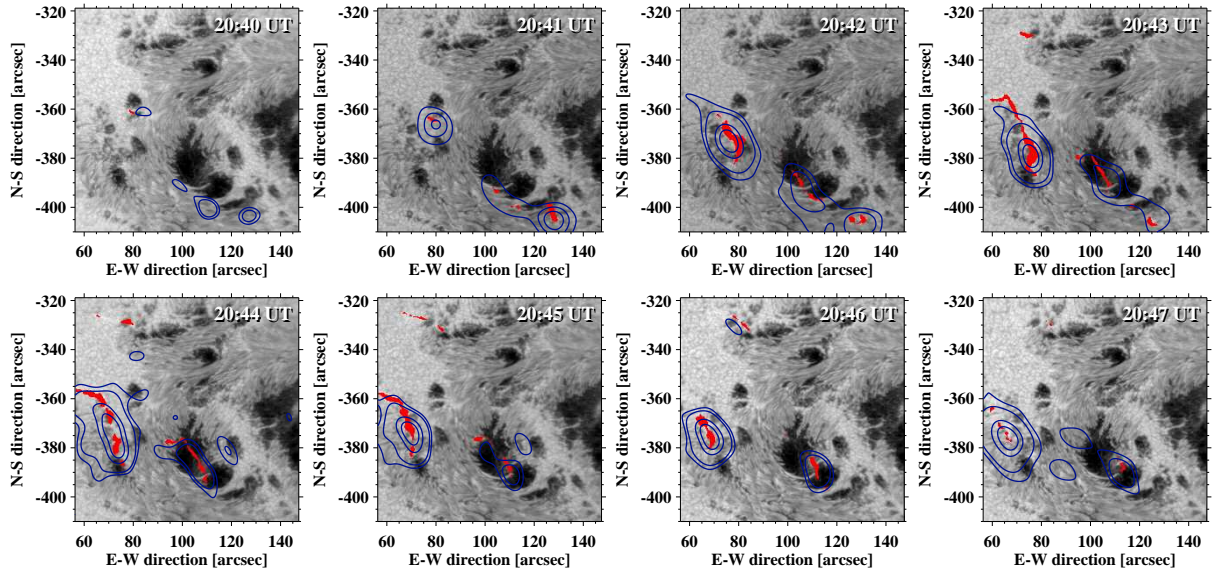


Figure 8: NIR time sequence of the X10 flare from 20:40 UT to 20:47 UT on 2003 October 29. RHESSI HXR contours (blue) correspond to the 50 - 100 keV channel with 60 integration. The local NIR intensity maxima are shown in red. Two flare ribbons are correlated with strong HXR kernels. HXR contour levels are drawn at 0.17, 0.25, 0.60, and 0.80 of the maximum intensity, except for the first two frames, where they correspond to 0.7 and 0.8 for the first frame and 0.4, 0.6, and 0.8 for the second, when the HXR kernels were weaker.

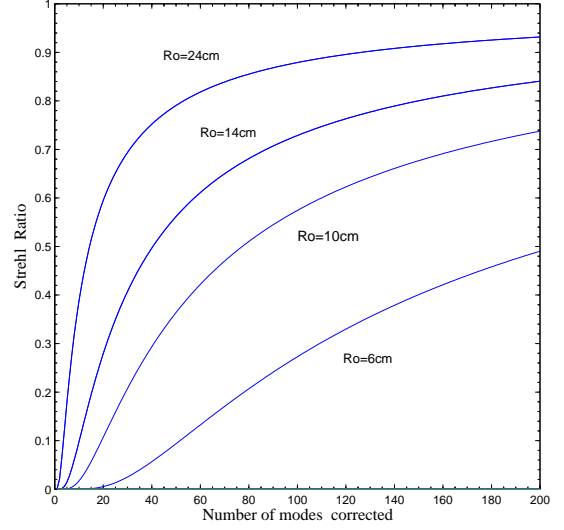
### A.2.3. Dynamics of Kilogauss Flux Tubes

One of the major breakthroughs in solar physics during the last 40 years has been the discovery that most photospheric magnetic flux that is measurable in visible light, via Zeeman polarization, appears outside of sunspots in the form of small scale flux concentrations with field strengths of typically 1 to 2 kG. Evolving from this discovery is the picture of small fluxtubes with typical sizes of a few tens to a few 100 kilometers, as building blocks of plage and network magnetic fields. Sophisticated Magneto-HydroDynamic (MHD) models now offer a variety of predictions that need to be tested. Also, precise measurements are necessary in order to define boundary conditions for these models.

The main questions about the dynamic behavior and structure of small scale kilo-Gauss fluxtubes, which need to be addressed with the 1.6-m telescope, concern the formation of photospheric flux concentrations with field strength above the equipartition field strength, and the dynamic interaction with the turbulent photospheric atmosphere. Understanding the dynamic interaction of photospheric flux concentrations with turbulent granulation is also essential in order to estimate the total energy flux that is transmitted/channelled by small-scale fluxtubes into the higher atmosphere. The key questions are: How are fluxtubes formed and how do they evolve? What is the lifetime of a fluxtube? How do the fluxtubes interact with turbulent flows in the photosphere? The observational verification of the process(es) that leads to kilo-Gauss flux concentration in the solar photosphere, where the equipartition field strength is only about 500 G, is a fundamental problem in solar and stellar physics that needs to be solved, and 50 to 100 km resolution is critical to resolve this problem. Although the AO supported observations in NIR can not achieve highest resolution of NST in visible, NIR observations do have a prominent advantage over the visible: the seeing conditions are more stable, therefore, the evolution of fluxtubes can be studied more accurately, with a resolution of 150km.

As a final remark of the scientific objectives, the scientific results will be extremely important to the

Figure 9: Theoretical Strehl ratio as a function of the corrected modes at different seeing conditions:  $r_0=6$  cm, 14 cm and 24 cm are the BBSO median seeing at 0.5, 1.0 and  $1.6\mu\text{m}$  respectively. In addition, a curve for  $r_0=10$  cm is included for the discussion in the proposal.



understanding of dynamics of magnetic fields in the fine spatial scale, as well as space weather monitoring and forecasting. The research will also be closely linked into several key research topics in nighttime astronomy: the physics of stellar coronal heating, stellar magnetic fields and stellar flares, as the sun is the only star that its detailed structure can be revealed.

### A.3. The Technical Detail of the AO project for the 1.6-m NST

As discussed above, with its 1.6-m aperture, the performance of the NST could be significantly improved if an AO is available to correct the wavefront errors caused by atmospheric turbulence, telescope alignment and possible mirror figure errors. We will develop a new AO system for the NST, which is re-tailored from the current AO system of the 65-cm telescope. The current AO-76 is one of the most successful solar AO systems in the world and is delivering excellent diffraction-limited images in the visible and NIR with the BBSO 65-cm telescope (Rimmele et al. 2003, Ren et al. 2003a, Didkovsky et al. 2003, Tritschler et al., 2005). Previous experience plus crucial hardware and software components that are in hand give us enough confidence and ability to transfer it to the NST.

#### A.3.1. Evaluation of the Strehl Ratio

The AO design parameters are driven by the seeing conditions at the site. In general, the seeing (Fried) parameter  $r_0$  is used to quantify the seeing conditions at a site.  $r_0$  is the coherence length of the atmospheric turbulence. For telescope apertures larger than  $r_0$ , the resolution is limited by seeing. The Fried parameter is wavelength dependent ( $r_0 \propto \lambda^{\frac{5}{3}}$  for Kolmogorov turbulence).

As stated above, the NST has an aperture that is about three times that of the current 65-cm telescope. Thus the AO system could fully correct the atmospheric turbulence at  $1.6\mu\text{m}$  in the NIR, meanwhile, for the visible wavelengths, it could partially correct the turbulence under good seeing condition. The median seeing at the BBSO is about  $r_0=6$  cm at  $0.5\mu\text{m}$ , while it is 24 cm at  $1.6\mu\text{m}$ . The 24 cm seeing is well-sampled by the Deformable Mirror (DM) and Wave-Front Sensor (WFS) lenslet array, both of them have 10 elements across the pupil. Let us look at the details.

The Strehl (S) ratio, which is the ratio of the maximum intensity in the AO corrected image to that in the diffraction limited image, is generally used to quantify the AO system performance. Figure 9 plots the expected Strehl ratio vs. number of corrected modes, using  $r_0$  as a parameter. It did not consider the noises in the images obtained by the WFS. As can be inferred from the theoretical Strehl ratios in Figure 9, even moderate variations in  $r_0$  will result in large variations in Strehl, if only a small number of Zernike modes are

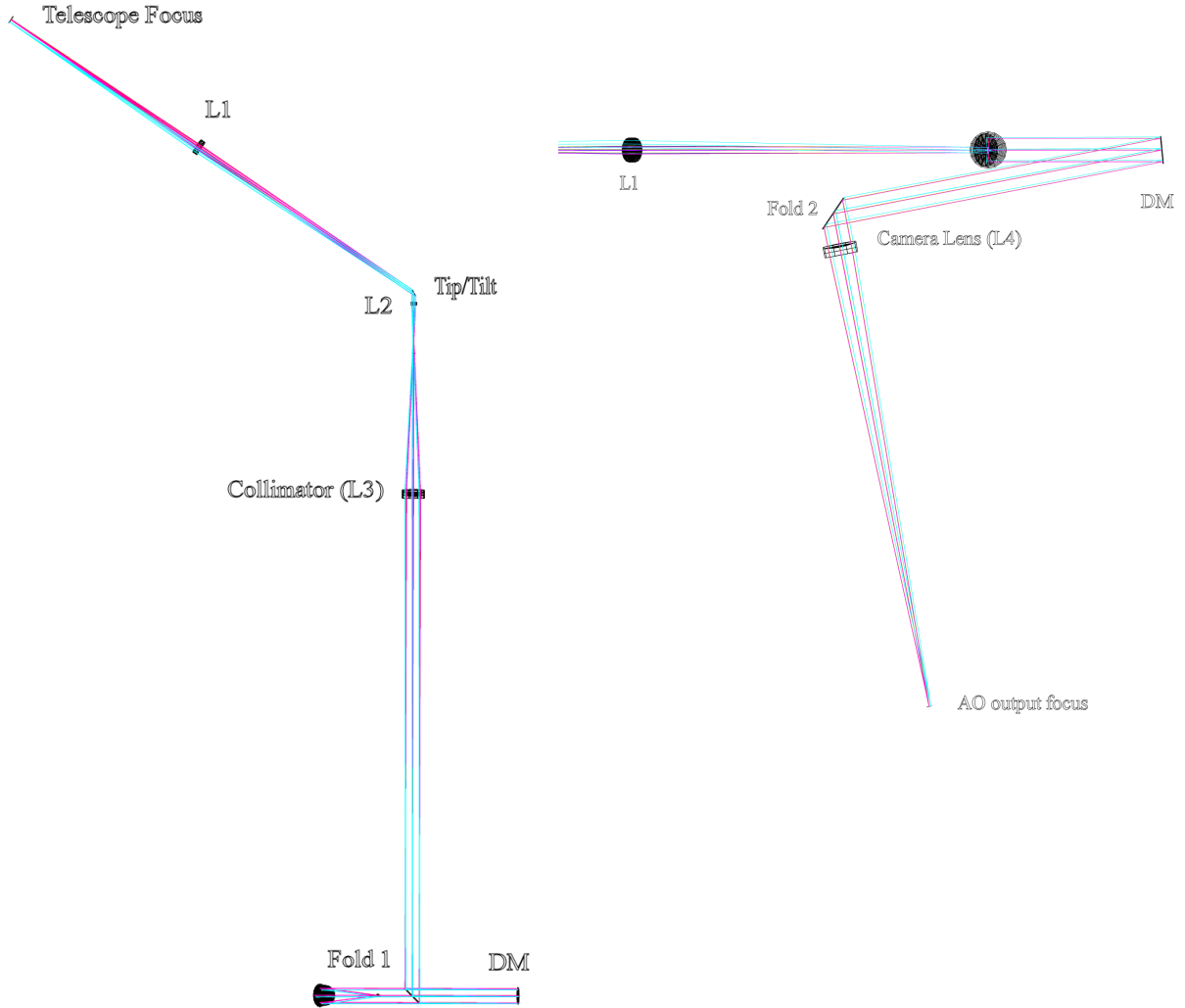


Figure 10: The schematic conceptual optical lay-out of one of possible designs for the NST AO system. Left is the side view of the layout: the NST pupil is first imaged onto the tip/tilt mirror by the lens L1. The solar image is then collimated and the telescope pupil is re-imaged again onto the DM by Lenses L2 and L3. Finally, at the AO output, a real solar image is formed by lens L4, which could be fed to science instruments. which is viewed from a vertical direction to that of the side view; Right: the top view of the optical layout.

corrected. This is mostly due to the correlation fitting errors while calculating relative image shifts for the sub-apertures in the WFS, which increases as  $r_0$  decreases. Also, a higher bandwidth (correction frequency) is required as the seeing gets worse.

From Figure 9, at  $1.6\mu m$ , when the median  $r_0$  is 24cm, 76-mode correction would achieve a Strehl ratio of 0.84. While in visible at  $0.5\mu m$ , the median  $r_0$  is 6cm, the corresponding Strehl ratio is 0.18. However,  $r_0$  above 10 cm is quite common at BBSO. Under the later conditions, we can achieve a Strehl ratio above 0.5. In summary, at least 50% of observing time, the achieved AO correction Strehl ratio at  $1.6\mu m$  is above 0.84; at  $0.5\mu m$ , 10% of observing time will have a Strehl ratio above 0.5.

### A.3.2. Overview of the AO Development Effort

Conceptually, of the AO is very straightforward: A beam splitter directs a light beam to the wavefront sensor (WFS) that will do the following: The telescope aperture is sampled by an array of lenslet, which in turn forms an array of images of the object (e.g. granulation) to be imaged by a camera with kHz frame rate.

Cross-correlations between subaperture-images and a selected reference subaperture-image are computed via a very fast computer-Digital Signal Processor (DSP). Local wavefront tilts are computed by locating the maximum or centroid of the cross-correlations (CC) to subpixel precision. Drive signals for the Deformable Mirror (DM) are derived from the wavefront sensor data using a modal wavefront reconstruction algorithm (e.g., Madec 1999). This WFS is capable of using solar granulation, or other time varying, low contrast, spatially extended targets to measure the wavefront aberrations. The current bandwidth of the correction is 135Hz in the closed-loop mode.

Due to the vastly different image scales of the 1.6-m NST and the current 65cm telescope, the optics will have to be re-designed to ensure that the pupil of the NST is correctly imaged onto the DM and the WFS lenslets with the correct size. Furthermore, the new optics would also be needed to relay the NST image from the telescope focal plane at the dome to the observing room 10-m below where the scientific instruments are located. The WFS optics will also be re-designed to reflect the change in the image scale. The rest of the current AO-76 system, such as the tip/tilt mirror, DM, electronics (including DSPs), WFS (except for wave-front optics), and some of the mechanical mounts could be used for the new AO system.

The wave-front sensor is a correlation Shack-Hartmann WFS. The WFS is designed to be able to process up to 80 sub-apertures. The wave-front sensor detector is a Baja CMOS 10-bit camera which has  $1280 \times 1024$  pixels. We achieve a frame rate of 2487 fps, using a  $200 \times 200$  sub-array. The small ( $D=30\text{mm}$ ) tip/tilt mirror is mounted on a Polytec PI S-330.30 piezo tilt platform, and the DM was manufactured by Xinetics, Inc. The WFS has 76 effective elements while the DM has 96 actuators.

### A.3.3. Optical Design

Since the current AO system needs to be transferred to the new NST, the major work involves a re-design and construction of the optics. We are very confident about the AO design, as Co-PI Ren designed both existing BBSO and NSO AO systems. He will be in charge of this new design work. There are some requirements for the optics of the new NST AO system: the optics must relay the NST focal plane image to the Coude room (a room one floor beneath the telescope) that is over 10m below the NST focal plane; the field-of-view for the optics must be  $180''$  in diameter, so that wide field observations will be possible. The initial design will be optimized at the near infrared for the wavelength range of 0.9 to  $1.6\mu\text{m}$ , but has an acceptable results in the visible.

To deliver excellent optical performance, some of the optical components in the AO relay path might be custom-designed and made. Figure 10 shows the optical layout of a possible initial design for the new AO main optical path which does not include the WFS. The NST pupil is first imaged onto the tip/tilt mirror with a small beam size of  $\sim 30\text{mm}$  diameter by the lens L1. The small pupil size is needed so that the small fast tip/tilt mirror can be used. The  $180''$  field-of-view is decided by the field stop in the telescope. However, the sun is re-imaged after tip/tilt mirror by lens L2 where a field stop could be located to select a smaller field of view. The solar image is then collimated by lens L3 and the telescope pupil is re-imaged again onto the DM with an 80-mm beam size. Finally, at the AO output, a real solar image with  $f/50$  focal ratio is formed by lens L4, which could be fed to science instruments. The fold mirrors (Fold 1 and 2), DM, camera (Lens 4) and WFS are all located on a horizontal optical bench so that the alignment can be done conveniently.

If we choose a refractive system as shown in Figure 10, all the lenses will consist of three optical materials FK51/BK7/FK51. The FK51/BK7/FK51 triplet was successfully used in our previous AO design (Ren et al. 2003a) and is a good choice to correct possible chromatic aberrations over a wide wavelength range. The triplets are commercially available from vendors such as Optical Components Inc. Figure 11 is the spot diagram of the main AO optical path over the entire  $180''$  field of view for the design is Figure 10. The optical performance is close to diffraction-limited over the entire wavelength range ( $0.9 \sim 1.6\mu\text{m}$ ). The dominant optical aberration over the wide wavelength range is, of course, the chromatism. However, most of our scientific goals will be achieved in certain narrow wavelength range for each specific observing run.

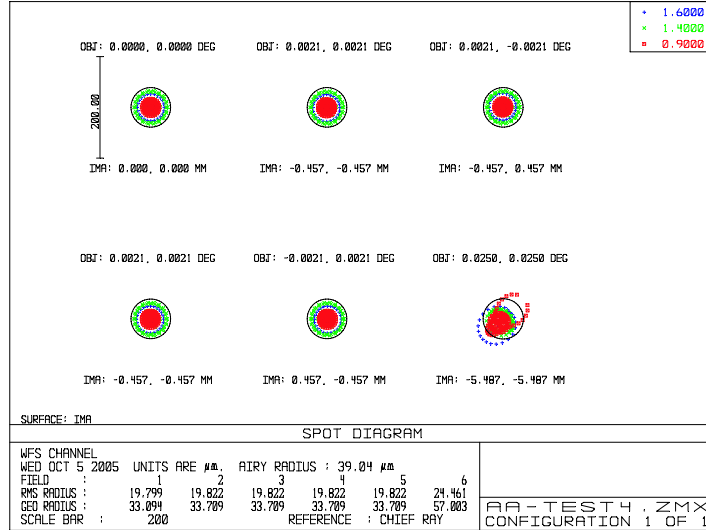


Figure 11: Spot diagram of the AO’s main optical path based on the design option shown in Figure 10. The circles are Airy disk. The optical performance is close to diffraction-limited at the entire 0.9~1.6 $\mu\text{m}$  wavelength range.

The chromatism is not a big concern, as long as the optical setup is checked and re-calibrated before each change of observing wavelength range.

A cubic beam-splitter will be located in the collimated beam between the DM and Fold 2, so that part of the light ( $\sim 5\%$ ) is used for wave-front sensing. Since WFS works in a very narrow waveband ( $\sim 10\%$  of the wavelength) in the visible, commercial in-stock lenses could be used and the chromatism would not be a concern. With moderate modification for the optics by change the re-imaging lenses, the current WFS could be used for the NST’s new AO system.

Design	Refractive	Reflective
Transmission	Lower	Higher
Complexity and the Size of the System	Simpler and Smaller	More Complicated and Larger
Chromatic Abberation	A Major Issue	None
Instrument Polarization	Less Significant	More Significant

Table 1: Comparison of Advantages and Disadvantages of the refractive and reflective designs.

As we stated clearly, the presented AO design is only one of the options that we will develop once this proposal is funded. We will certainly consider the all reflective system. Table 1 compares the trade-offs between the reflective and refractive systems. Each has some limitation. As part of our design effort, we will present a few designs for the refractive and reflective systems. We anticipate that in the end, we may construct a system with a combination of lenses and mirrors to optimize the performance.

Finally, the wave-front error of the entire AO system will be tested by using a single-mode fiber interferometer, which was developed by one of the Co-PIs (Ren et al. 2003b). The wave-front error test will also be done by using the fiber interferometer, so that the alignment error could be minimized. We will also use the interferometer to calibrate the WFS.

### A.3.4. Electronic, Computing and Mechanics Systems

As we already stated, the main system components for the AO system are:

- a correlating Shack-Hartmann WFS

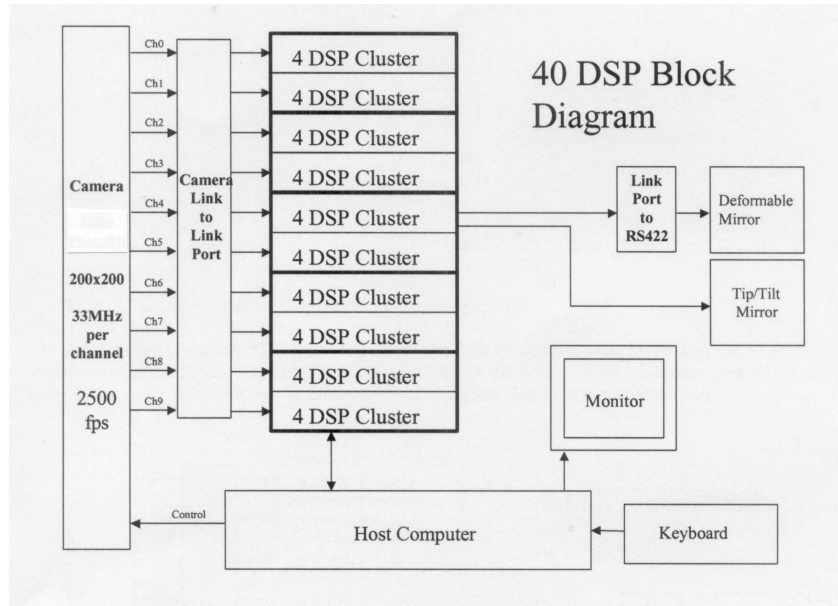


Figure 12: Functional block diagram of WFS and the reconstruction unit of the AO-76 system (Rimmele et al. 2003).

- a wavefront reconstructor
- a deformable mirror(DM).

Figure 12 shows the block diagram of the hardware that are basically applicable to the existing and the new AO. Although most of the electronic components will be transferred to NST, we anticipate that the software will need to be revised. Dr. John Varsik will be in charge of the software development, and handling of electronic system. Among many issues of software development, the reconstruction matrix needs to be modified to reflect the entrance pupil difference between the 65-cm telescope and the NST. Co-PI Ren will provide the calculation of the matrix, to be implemented by Dr. Varsik. The mechanical system for the AO will be modified and fabricated by Jeff Nenow.

### A.3.5. Setup, Testing and Observations of the New AO System

In Table 2, we list the major proposed tasks of this AO project. The main tasks of year 1 will be the optical and mechanical designs of the AO system and then the interface to the focal plane instruments. NST will be installed in the middle of the first year. The main tasks of the second year will be to set up the AO system; analyze WFS data and observe with new focal plane instrument, in particular, the IRIM system. The setup, testing and observing with the system will have the following components and will be carried out mainly by Wenda Cao, a post-doctoral associate and Dr. Ren:

- The optical design may be modified further during the testing of the AO system, if it is needed.
- The NST will use 42-actuator active mirror system. AO-76 will be used to evaluate telescope aberrations by averaging WFS data over a set time period. This will provide a initial lookup table for the active mirror system, and evaluate the change of aberrations when the NST is moving to point at different directions, or under different thermal conditions.
- It is well-known that for a regular AO system, the high bandwidth correction requirement allows only partial correction. Also AO is not so effective for large fields of view because of anisoplanatism. The solution is to post-process the data in subfields smaller than the anisoplanatic angle, which for many applications is on the order of  $5''$ . The problem is to separate the object and the aberrations, two unknown quantities, in

the images in the presence of noise, a third unknown. To obtain correction in larger field of view, BBSO is developing Phase Diversity (PD) system. PD utilizes a model of the image formation process to constrain the estimation of the aberrations and the common object in two image channels with a known difference in the pupil phase, usually a focus shift. An image collected in this second optical channel will contain the effects of the unknown phase aberrations, but will also be influenced by the intentional defocus, which adds a known quadratic phase. Obviously, the phase information from PD system will help us to analyze the wave front information of the AO system.

(d) As the IRIM will be our initial science instrument to work with NSO and the new AO system, it must be in a very mature stage before the end of the first year. Dr. Cao will work on this system, to be tested with the current AO at BBSO and NSO/SP, then to be integrated it to the new AO.

(e) A key component in the AO development is to analyze the wavefront data to evaluate the operation of the AO, and guide the modification of the system. Co-PI Prof. Denker will lead this effort as he has gained significant experience in analyzing the current BBSO AO data (Tritschler et al., 2005).

Year	Task	Person In Charge
Year 1	Overall Management and Science Direction	Wang
	Interface with NST	Goode
	General Technical Advising and Design Review	Rimmele
	Optical Design	Ren
	Software and Electronics	Varsik
	Mechanical Design and Fabrication	Nenow
	Wavefront Data Analysis for Current AO	Denker
	Finalize IRIM	Cao
Year 2	Overall Management and Science Direction	Wang
	Interface with NST	Goode
	General Technical Advising	Rimmele
	AO setup and test	Ren, Cao, Varsik
	Optical Design Modification	Ren
	Software and Electronics	Varsik
	Mechanical Fabrication and Modification	Nenow
	Wavefront Data Analysis for New AO	Denker
IRIM Observation with AO	Cao	

**Table 2:** Tasks and Assignments for the Proposed AO Project.

## A.4. Relationship to Future Work and Night-time Astronomy

### A.4.1. Higher Order Solar AO in the Future

After the NST is fully operational with the proposed AO-76, we will then explore extending the full AO correction down to visible wavelengths. Obviously, there are many important spectral lines in the visible for the solar observations. In addition, the diffraction limit in the visible is three times smaller than that at NIR, so higher spatial resolution will be achieved if we can obtain full AO correction in the visible. We acknowledge that such an AO system would require a larger number of DM actuators, WFS sensing elements and fast DSPs, but the scientific returns are also greatly enhanced. This will be a challenging task and require substantial new funding that we will seek in the future. However, working with AO-76 on NST is an essential step to help us to gain the experience to upgrade the AO in the future. For example, with the proposed upgrade, we will study wavefront based on WFS data to characterize the local turbulence properties and to decide how many elements will be needed for the higher order AO.



#### **A.4.2. Multi-Conjugate AO**

The project is also an essential step to enable us to explore Multi-Conjugate Adaptive Optics (MCAO) further down the road. MCAO is a further development of the AO concept, where the correction is made by several DMs conjugated to different altitudes. While MCAO is a promising technique for atmospheric turbulence correction over a large field of view (Ragazzoni et al. 1999, Tokovinn, A. et al. 2001, Ellerbroek et al. 2003), night-time MCAO is difficult for wave-front sensing, since multiple laser guide stars are needed for the tomographic wave-front reconstruction. To accurately reconstruct the 3-D turbulence, generally at least 3~5 laser guide stars are needed. Due to this and other difficulties, there is no any night-time MCAO is in operation currently. The sun is a natural target for extended object wave-front sensing, any number of “target stars” could be made from the 2-dimensional structure of the sun by using correlation Shack-Hartmann wave-front sensing technique: a technique being using in our solar AO system. This provides an excellent opportunity to develop the MCAO. Once this proposal is funded, we plan to build a dedicated WFS which would allow wave-front sensing over a large field of view. The large field could be further divided into many sub-field for tomographic wave-front sensing. Data from such a wide field WFS could be collected and the 3-D tomographic wave-front turbulence could be constructed, which would eventually allow us to simulate and estimate the possible performance that is achieved for an MCAO system.

### **B. Education and Research Training**

BBSO currently has fifteen Ph.D. students (including 5 US and 3 female students) who will receive Ph.D.s from NJIT in various fields, ranging from applied physics to electrical and computer engineering to computer science. The very best NJIT students are attracted to the BBSO program. The typical student designs and builds the instruments used to make his/her Ph.D. measurements in BBSO. These students utilize the laboratories and our small observatory on campus to test the instruments for use at BBSO. BBSO also supports 2-3 undergraduate students for summer research at Big Bear.

Although we do not seek additional funding for students in this proposal, one of the Ph.D. students and an undergraduate student supported by BBSO’s operation budget will be assigned to the project. We believe that this project will be a strong draw for talented NJIT students who are already interested in instrument development.

### **C. Personnel and Management**

As the project is relatively small, PI Wang will also act as the Project Scientist/Project Manager to monitor the progress of the project and ensure the proper connection between instrumentation and scientific return. He will coordinate with the NST Project Manager, Roy Coulter. Co-PI Goode will oversee the integration of the AO system and the NST, as he is the PI of the NST project. Co-PI Denker will participate in the design of optical system and analyze WFS data. Wang, Denker and Goode will not charge this grant as they are paid as regular faculty members. The proposed budget will cover 50% of Co-PI Ren’s salary, and 50% of salary of a post-doc, Wenda Cao, 25% salary of Varsik, a research professor, plus 20% of salary of Jeff Nenow, the mechanical engineer at BBSO. Dr. Rimmele will participate in the project under the role of general advising and reviewing of designs, using his profound experience in AO projects. The hardware cost of the project is around \$50k.

## D. References

- Cao, W., Jing, J., Ma, J., Xu, Y., Wang, H. and Goode, P.R., 2005, *Diffraction Limited Polarimetry from Infrared Imaging Magnetograph of Big Bear Solar Observatory*, Ap.J. Letters, submitted.
- Denker, C., Mascarinas, D., Xu, Y. Cao, W., Yang, G., Wang, H., Goode, P. R. and Rimmele, T., 2005, *High-Spatial-Resolution Imaging Combining High-Order Adaptive Optics, Frame Selection, and Speckle Masking Reconstruction*, Solar Physics, 227, 217-230
- Didkovsky, L., Dolgushyn, A., Marquette, W., Hegwer, S., Ren, D. Fletcher, S. Richards, K., Rimmele, T. R. Denker, C. and Wang, H. 2003, "High-order adaptive optical system for Big-Bear Solar Observatory," Proc. SPIE, 4853, 630-639
- Ellerbroek, B. E. Giles, L. and Vogel, C. R. 2003, "Numerical simulations of multi-conjugate adaptive optics wave-front re-construction on giant telescope," Applied Optics, 42, 4811
- Goode, P. R., Denker, C. J., Didkovsky, L. I., Kuhn, J. R. and Wang, H., 2003, "1.6 M Solar Telescope in Big Bear – The NST", JKAS, 36, 125-133
- Hill, F. et al., 2004, ATST Site Survey Report
- Ji, H., Wang, H., Schmahl, E. J., Moon, Y.-J.; Jiang, Y. 2003, *Observations of the Failed Eruption of a Filament*, Ap.J. Letters, 595, 135-138
- Ji, H., Wang, H., Schmahl, E. J., Qiu, J. and Zhang, Y., 2004a, *Observations of Nonthermal and Thermal Hard X-Ray Spikes in an M-Class Flare*, Ap.J., 605, 938-947
- Ji, H., Wang, H., Goode, P. R., Jiang, Y. and Yurchyshyn, V., 2004b, *Traces of the Dynamic Current Sheet during a Solar Flare*, Ap.J. Letters, 607, L55-58
- Lin, H., Kuhn, J.R. and Coulter, R., 2004, *Coronal Magnetic Field Measurements*, Ap.J., Letters, 613, L177-180
- Liu, C., Deng, N., Liu, Y., Falconer, D., Goode, P. R., Denker, C. and Wang, H., 2005, *Rapid Change of delta Spot Structure Associated with Seven Major Flares*, Ap.J., 622, 722-736
- Madec, P.Y., 1999, in *Adaptive Optics for Astronomy*, F. Roddier ed., Cambridge University Press, 131
- Rimmele, T. R., 2004 *Recent advances in solar adaptive optics*, 2004, SPIE, 5490, 34
- Qiu, J., Ding, M. D., Wang, H., Gallagher, P. T., Sato, J., Denker, C., and Goode, P. R., 2001, *Ultraviolet and Halpha Emission in Ellerman Bombs*, ApJ Letters, 554, L445-448
- Qiu, J., Lee, J. W., Gary, D. E., and Wang, H., 2002, *Motion of Flare Footpoint Emission and Inferred Electric Field in Reconnecting Current Sheets*, Ap.J., 565, 1335-1347
- Qiu J., Hurford, G. and Wang, H., 2005, *Fine Temporal Structure of Solar Flares*, Ap.J., submitted
- Ragazzoni, R., Marchetti, E. and Rigut, F., 1999, *Modal Tomography for Adaptive Optics*, A&A, 342, L53-56
- Ren, D., Hegwer, S. and Rimmele, T. R. et al. 2003a, "The optical design of a high order adaptive optics for the NSO Dunn solar telescope and the Big Bear solar observatory", Proc. SPIE, 4853, 593

- Ren, D., Rimmele, T., Hegwer, S. and Murray, L. 2003b, "A single-mode fiber interferometer for AO wavefront test", *PASP*, 115, 355-361
- Rimmele, T. R., Richards, K., Hegwer, S. L., Ren, D., Fletcher, S., Gregory, S., Didkovsky, L. V., Denker, C. J., Marquette, W., Marino, J., Goode, P. R. 2003, "Solar adaptive Optics: a Progress Report", *Proc. SPIE*, 4839, 635
- Spirock, T., Yurchyshyn, V., and Wang, H., 2002, *Rapid Changes in the Longitudinal Magnetic Field Related to the 2001 April 2 X20 Flare*, *Ap.J.*, 572, 1072-1076
- Sturrock, P. A., 1989, *Proceedings of Max'91 Workshop*, p. 1
- Tokovinn, A. et al. 2001, "optimized modal tomography in adaptive optics," *A&A*, 378, 710
- Tritschler, A., Denker, C., Rimmele, T., Richards, K and Hegwer, S., 2005, "The High-Order Adaptive Optics System at the Big Bear Solar Observatory", *Solar Physics*, submitted
- Wang, H., Qiu, J., Denker, C., Spirock, T., Chen, H., and Goode, P. R., 2000, *High-Cadence Observations of an Impulsive Flare*, *ApJ*, 542, 1080-1087
- Wang, H., Spirock, T. J., Qiu, J., Ji, H., Yurchyshyn, V., Moon, Y.-J., Denker, C. and Goode, P. R., 2002, *Rapid Changes of Magnetic Fields Associated with Six X-Class Flares*, *Ap.J.*, 576, 497-504
- Wang, H., Liu, C., Qiu, J., Deng, N., Goode, P. R., & Denker, C., 2004, *Rapid Penumbra Decay Following Three X-Class Flares*, *Ap.J. Letters*, 601, L195-198
- Xu, Y., Cao, W., Liu, C., Yang, G., Qiu, J., Jing, J. Denker, C. and Wang, H., 2004, *Near-Infrared Observations at 1.56 Microns of the 2003 October 29 X10 White-Light Flare*, 2004, *Ap.J. Letter*, 607, L131
- Xu, Y., Cao, W., Liu, C., Yang, G., Jing, J., Denker, C., and Wang, H., 2005, *High Resolution Observations of Multi-Wavelength Emissions During Two X-Class White-Light Flares*, *Ap.J.*, Submitted
- Yang, G., Xu, Y., Cao, W., Wang, H., Denker, C. and Rimmele, T. R., 2004, *Photospheric Shear Flows Along the Magnetic Neutral Line of Active Region 10486 Prior to An X10 Flare*, 2004, *Ap. J. Letters*, 617, L151-154